Energetic coefficient of friction applied to cylinder liners lab tests

Joao Luiz do Vale
Surfaces and Contact Lab. (LASC), UTFPR – Universidade Tecnológica Federal do Paraná, Londrina, Brazil, and
Carlos Henrique da Silva and Giuseppe Pintaude
Surfaces and Contact Lab. (LASC), Universidade Tecnológica Federal do Paraná, Curitiba, Brazil

Abstract

Purpose – This paper aims to present a proposal for evaluating the coefficient of friction (*COF*), under a reciprocating test that considers the energy dissipated by the friction force. In addition, this new parameter is compared to average *COF*, which is often used to evaluate *COF* in reciprocating tests.

Design/methodology/approach – Samples of compacted graphite iron were extracted directly from an internal combustion engine block. The piston ring used was a nitrided martensitic stainless steel with an asymmetrical profile, and the lubricant oil was the SAE 30 CF, controlled at 40°C. Different testing conditions were carried out in a CETR-UMT-Bruker tribometer, varying loads between 25-125 N, frequencies between 1-12.5 Hz and track length between 3-10 mm. Three maps comparing the average *COF* and the energetic definition were built, allowing to discuss their similarities.

Findings – In general, both parameters had similarities especially for low frequencies and small tracks. However, for test conditions that imposed higher accelerations (i.e. longer track lengths and higher frequencies), the energetic *COF* (*COFe*) was lower than the average *COF* (*COFa*) and presented better agreement in Stribeck-like curves – independent on the experienced lubrication regime along the stroke. As the *COFe* can be interpreted as a weighted average of instantaneous *COF* in relation to in-track displacements, an immediate consequence is that instantaneous *COF* closest to mid-stroke is considered more significant. Furthermore, perturbations associated with the intrinsic accelerations of the movement test are minimized in the *COFe* formulation.

Originality/value – The energetic *COF* parameter (*COFe*) is presented and compared to the average *COF*. The new parameter presented less data dispersion and is attractive to evaluate the *COF* behavior in reciprocating tests, as its formulation minimizes perturbations associated with the intrinsic accelerations of the movement (mainly in the initial and final part of the track where the acceleration has its greatest magnitude).

Peer review – The peer review history for this article is available at: https://publons.com/publon/10.1108/ILT-08-2019-0324

Keywords Coefficient of friction, Cylinder liners, Data processing, Energetic approach, Reciprocating test

Paper type Research paper

Nomenclature

COF = coefficient of friction [-];
COF_a = average coefficient of friction [-];
COF_e = energetic coefficient of friction [-];
COF_i = instantaneous coefficient of friction [-] ;
CV = coefficient of variation [-];
E = energy dissipated by the friction force [J];
F = frequency [Hz];
f_i = instantaneous friction force [N];
i = an instantaneous data collected [-];
n = total number of data collected [-];
N = normal force [N];
N_i = instantaneous normal force [N];
SD = standard deviation [10^{-3}];
Str = stribeck parameter [m];
Sq = root mean square height [μm];
TL = track length [mm];
$\boldsymbol{V_i}$ = instantaneous sliding velocity [mm/s];
$\boldsymbol{x_i}$ = instantaneous position [mm];
Δx_i = instantaneous displacement [mm]; and
η = oil kinematic viscosity [cP].

1. Introduction

Friction is an important issue for transportation and specifically for the internal combustion engines industry. Following Holmberg and Erdemir (2017), considering transportation, 75 per cent of global transport energy use are due to road vehicles. Previously, Holmberg *et al.* (2012) estimated 11.5 per cent of

The current issue and full text archive of this journal is available on Emerald Insight at: **https://www.emerald.com/insight/0036-8792.htm**

Industrial Lubrication and Tribology
72/9 (2020) 1103–1108

[DOI 10.1108/ILT-08-2019-0324]

The authors would like to thank the support given by Tupy S.A. for the financial support through the cooperation ACT 10/2015 TUPY-UTFPR, and for Mahle Metal Leve S.A. for providing the samples of piston rings. One of authors, G. Pintaude, thanks to CNPq by the financial support through Process 308416/2017-1.

Received 10 August 2019
Revised 23 October 2019
Accepted 30 November 2019

the losses due to the friction in vehicles supplied 100 per cent by fuel energy. The combination of these numbers gives rise to an impressive effect of friction for saving consumption and, consequently, reducing the emissions.

Because of that, different lab approaches are available for reproducing the piston ring-cylinder liner contact, aiming to measure the coefficient of friction (*COF*) for this relevant tribological pair. Three approaches certainly are amongst the most used in the literature:

- dynamometry (Tomanik, 2008);
- pin-on-flat configuration in a reciprocating system (Maru and Tanaka, 2007); and
- ring-on-cylinder in a reciprocating system (Vale *et al.*, 2018).

Recently, another one was proposed by Dimkovski *et al.* (2018) to reproduce velocities closer to those experienced in a real engine.

Specifically, in the lab rigs that made use of the reciprocating movement, some issues are of great importance for determining the *COF*. Although the reversal points in the reciprocating lab test rig reproduce the movement in a real engine, they represent sources of instabilities since high-velocity variations are present. In this context, the current investigation analyzes the possibility of another approach for the COF can be more suitable for the reciprocating system than a simple average value.

2. Materials and methods

2.1 Materials

Cylinder samples were extracted from a diesel combustion engine manufactured in a compacted graphite iron (GJV 450, 220 ± 10 HV20), and their surfaces were honed in a two-step process for obtaining plateau finishing. Details of microstructure and honing variables were described elsewhere (do Vale *et al.*, 2017). An average value of 0.61 ± 0.05 μm for Sq roughness parameter was obtained from this cylinder manufacturing. Ring samples, by their turn, were extracted from a compression ring – manufactured in martensitic stainless steel and its contact surface was nitrided in an industrial process (1070 ± 40 $HV_{0.1}$) – with an asymmetric profile (an 83 mm nominal diameter and 1.2 mm thick). Due to its asymmetry, the results are presented keeping the direction of movement reference of the piston ring when it is assembled in the engine (i.e. upstroke and downstroke). The average *Sq* parameter of the piston ring surface is 0.55 ± 0.05 μm. Therefore, the equivalent roughness for the tribological pair is 0.82 μm.

During the tests, the samples were kept flood in a mineral oil SAE 30 CF whose temperature was maintained constant. This low additive package oil was chosen to avoid additives that eventually could influence on the friction behavior.

2.2 Tribometer and planning of tests

The data collected for evaluating the kinetic COF was obtained in a ring-on-cylinder configuration, schematically shown in Figure 1. The tribometer used was a CETR-UMT-Bruker. To minimize spurious data, a suspension was mounted to the ring sample holder.

Figure 1 Tribo-elements of the ring-on-cylinder reciprocating test

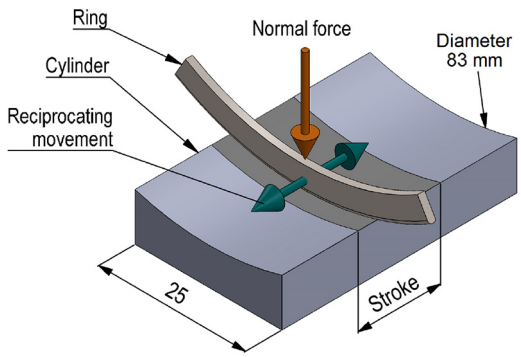

Source: Vale *et al.* (2018)

A load cell DFH-20 with a range from 2 to 200 N and resolution of 10 mN was used with data acquisition of 1 kHz. The output data for each collection event (i) were:

- the instantaneous values of position (x_i);
- the normal force (N_i); and
- the frictional force (f_i).

Thus, the instantaneous COF was obtained as $COF_i = f_i/N_i$. Figure 2 shows an example of the output data as a function of time. Note that the complete cycle of movement was divided into upstroke and downstroke semi-cycles. As the tribometer used is driven by a crank mechanism, x_i is a sinusoidal in-time function. Therefore, the instantaneous sliding velocity (V_i), which is proportional to the instantaneous displacement (Δxi), assume null value at the reversal points of movement and maximum value at the mid-stroke. Additionally, the maximum acceleration is experienced at the reversal points.

Table I shows the planning of the tests. A total of 120 conditions were performed as a result of different selection for the frequency, normal force and track length variables. Emphasis should be given to the aim of sweeping a wide operating range of the tribometer. The test sequence was arranged considering that the same area of both the ring and the cylinder (i.e. the same track length) was used for three different

Figure 2 Example of the tribometer's output data as a time function

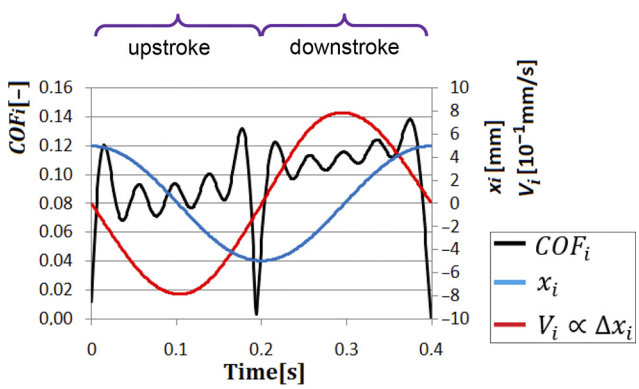

Notes: F = 2.5 Hz; N = 25 N and TL = 10 mm

Table I Planning of the reciprocating tests

List of parameters	List of values tested
Variable parameters (120 conditions)	
Frequency [Hz]	1.0 2.5 5.0 7.5 10.0 12.5
Normal Force [N]	25 50 75 100 125
Track lenght [mm]	3.0 5.0 7.5 10.0
Constant parameters	
Testing duration [*s*]	65
Period for data acquisition [*s*]	from 60 to 65
Oil temperature [°C]	40
Oil kinematic viscosity – 40° C [cSt]	92
Repetitions [–]	3

test conditions. This guarantees mild wear on the samples as well as statistically more representative data.

The testing duration was an important variable in this study. It must be kept in mind that even low additive package oils have in their composition anti-wear additives such as Zinc-dithiophosphate (ZDDP) (Spikes, 2004). Thereby, a few minutes of testing (approximately15min) is already enough for the tribofilm formation, imposing significant changes in the *COF* values (Kalin *et al.*, 2016). In contrast, a minimum testing duration is required to reach the steady state relative to the hydrodynamic lubrication regime. Only a few seconds of movement (about 40 *s*) are sufficient for this stabilization. Therefore, and taken both considerations together, the test duration was arbitrated as 65 *s* and data acquisition, to obtain *COF*, was taken only after 60 seconds (i.e. within the steady-state period).

2.3 Approaches for the coefficient of friction

This investigation compares two definitions for the COF, which intend to represent in a single value the behavior of the *COF* along a semi-cycle during the reciprocating movement. The first one, the average COF (COF_a) is a fairly usual parameter for researchers (Tomanik, 2008; Maru and Tanaka, 2007), defined in equation (1); where i and n represents, respectively, each collection event and the total number of data collected in a semi-cycle of movement:

$$COF_a = \frac{\sum_{i=1}^{n} \frac{f_i}{N_i}}{n} = \frac{\sum_{i=1}^{n} COF_i}{n} \quad (1)$$

The second one, the energetic COF (COF_e) is an approach proposed here as an alternative for evaluating the friction behavior. For this formulation, the energy dissipated by the friction force along a semi-cycle must be defined:

$$\mathrm{E} = \sum_{i=1}^{n} f_i.\Delta x_i \quad (2)$$

Further, to obtain the COF_e, two standardizations are imposed on the energy of semi-cycle, aiming to create a non-dimensional value. The instantaneous frictional force (f_i) is divided by the normal force (N_i) as well as the instantaneous displacements are divided by the sum of displacements. Thus, the ratio of forces is replaced by the instantaneous COF (COF_i) and the sum of the displacements is considered as the track length, *TL* [mm]. These operations are presented in equation (3):

$$COF_e = \sum_{i=1}^{n} \left(\frac{f_i}{N_i} . \frac{\Delta x_i}{\sum_{i=1}^{n} \Delta x_i} \right) = \frac{\sum_{i=1}^{n} COF_i.\Delta x_i}{TL} \quad (3)$$

Both the COF_a and COF_e were evaluated considering only the upstroke semi-cycles results - mainly due to the asymmetry of the piston ring. The *COF* values were obtained applying equations (1) and (3) for a single upstroke semi-cycle, starting immediately after 60 *s* of testing duration. This procedure was repeated 3 times.

Three comparisons between the results of the *COF* definitions were made. Maps were built for each track length, as a function of the normal force and the frequency, allowing the following comparisons:

- the percentage difference of friction definitions [equation (4)];
- the statistical similarity based on the Student *t*-test, with 95 per cent confidence level; and
- the standard deviation (*SD*) for both definitions:

$$\text{Percentage difference } [\%] = \left(1 - \frac{COF_e}{COF_a}\right).100 \quad (4)$$

Furthermore, the *COF* values were plotted on Stribeck-like curves whose formulation is presented in equation (5). The oil viscosity (η) was considered constant as shown in Table I. The maximum velocity of sliding (V_{max}) occurs in the mid-stroke as presented in Figure 2, and its magnitude depends on the frequency and the track length since the tribometer has a crank mechanism. The average pressure, in its turn, depends exclusively on the normal force applied:

$$Str = \frac{\eta \,.\, V_{max}}{P_{mean}} \quad (5)$$

The term P_{mean}, as the ring profile has no constant radius, was determined using a finite element analysis (Kalin *et al.*, 2016). For this purpose, a 2 D plane strain state was considered and the ring profile (obtained by interferometry) and the surface cylinder (considered as a plane) were modeled as smooth.

3. Results and discussion

3.1 Similarity and dispersion analyses

Figure 3 presents four maps of the relative percentage differences between the COF_e and COF_a. In some testing

Figure 3 Percentage difference maps of *COFe* in relation to *COFa*

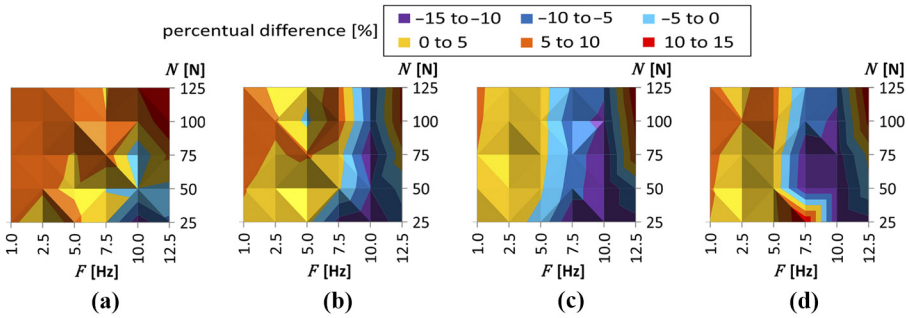

Notes: (a) *TL* = 3.0 mm; (b) *TL* = 5.0 mm; (c) *TL* = 7.5 mm; (d) *TL* = 10.0 mm

conditions, the values of the COF_e are higher (red tendency), but in the other ones, they are smaller (blue tendency).

Before analyzing the variations in the percentage difference presented in Figure 3, two considerations must be pointed out. Firstly, attention should be paid to the *COF* definitions, presented in equations (1) and (3). The COF_a simply represents a mean of all instantaneous COF (COF_i) obtained in a semi-cycle of motion. On the other hand, the COF_e is proportional to the sum of COFi Δxi, as presented in equation (3). With this, the sinusoidal in-time behavior of Δxi plays a key role in the COF_e parameter. As these displacements are proportional to the sliding velocity – as explained in Section 2.2 (Figure 2) – they assume null value at the reversal points of movement and maximum value at the mid-stroke. Therefore, COF_e can be interpreted as a weighted average of COF_i, concerning in-track displacements, with lower and higher weights for, respectively, reversal and mid-stroke points. An immediate consequence is that the COF_i obtained from the mid-stroke is considered more significant for the COF_e, than the other ones closer to the reversal points. Second, an extremely relevant consideration is that the reciprocating test has a self-excited vibration; making the output data susceptible to:

- perturbations associated with the intrinsic accelerations of the movement (mainly in the initial and final part of the track where the acceleration has its greatest magnitude); and
- the resonance phenomena related to the apparatus rigidity.

Based on the above-mentioned arguments, it is evident that the COF_e minimizes the critical perturbations associated with the reversal points, since these data have less weight in its formulation. In a tribometer driven by a crank mechanism, the major perturbation caused by acceleration is related to higher frequencies and higher track lengths.

Therefore, one can observe some testing conditions that impose minor acceleration, such as frequencies smaller than 7.5 Hz associated with track lengths of 3.0 and 5.0 mm. For these cases, Figure 3 shows that the COF_e is larger than the COF_a. On the opposite, in conditions that impose major accelerations, the percentage differences were placed between −10 and −15 per cent, demonstrating that the COF_a is more susceptible to these perturbations and has increased sharply, while the COF_e minimized this effect.

Despite the foregoing, 73.33 per cent of the testing conditions had statistically equal values of the COF_e and COF_a (with 95 per cent ~~of~~ confidence level), as shown in the correlation maps of Figure 4 – whose data are presented in the same way as Figure 3. Furthermore, most of those which did not have equality were associated with testing conditions that imposed major acceleration. Hence, these correlation maps show that the COF_e formulation is not always a new value describing the friction behavior along a semi-cycle, but rather it means a more robust formulation that minimizes the perturbations discussed in this section.

Another relevant evaluation for the *COF* definitions is their repeatability. For this purpose, Figures 5 and 6 provide the

Figure 4 Correlation maps between *COFe* and *COFa*

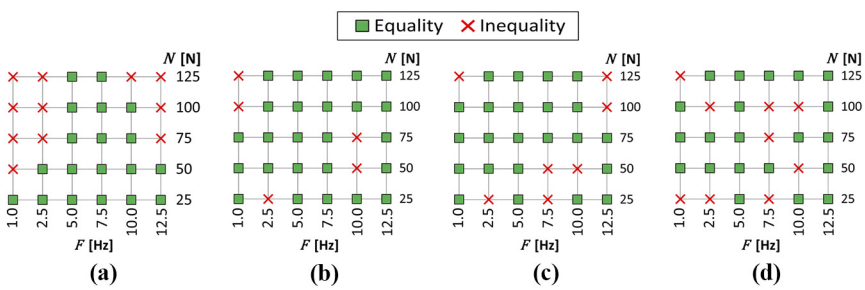

Notes: (a) *TL* = 3.0 mm; (b) *TL* = 5.0 mm; (c) *TL* = 7.5 mm; (d) *TL* = 10.0 mm

Figure 5 Map of standard deviation for *COFa*

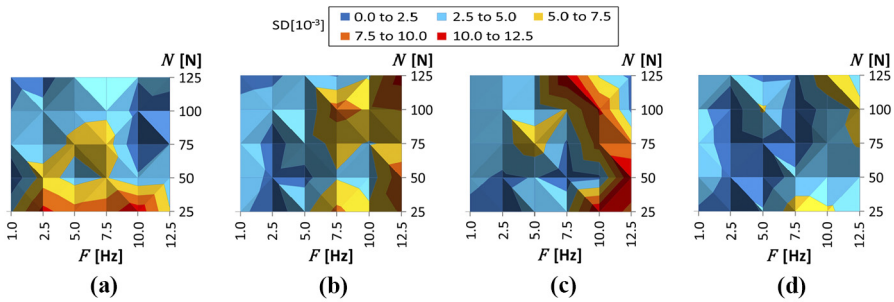

Notes: (a) TL = 3.0 mm; (b) TL = 5.0 mm; (c) TL = 7.5 mm; (d) TL = 10.0 mm

Figure 6 Map of standard deviation for *COFe*

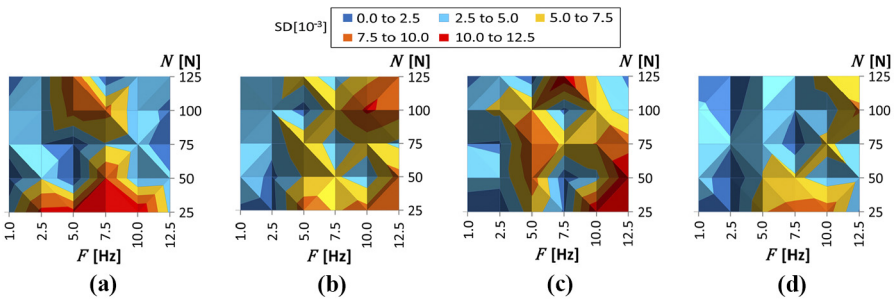

Notes: (a) TL = 3.0 mm; (b) TL = 5.0 mm; (c) TL = 7.5 mm; (d) TL 10.0 mm

standard deviations (SD [10^{-3}]) for the COF_e and COF_a, respectively.

In general, the results show a certain similarity between them and for the vast majority of test conditions SD < 7.5 – 77.50 per cent for the COF_e and 85.83 per cent for the COF_a – which shows that the repeatability for the parameters was the same. Logically, the evaluation of repeatability for reciprocating tests is not so simple. Taking into account the large range used for both the frequency and track lengths, it must be assumed that the resonance phenomena is more accentuated for certain conditions, leading to higher values of SD. Indeed, the values of SD for the COF_e and COF_a were placed in the range of 7.5 < SD < 10 (17 vs.10, respectively) for some cases, and of SD > 10 (10 vs. 7) for other ones. It should be emphasized that the scope of the current investigation is not to discuss the results and testing conditions under resonance. However, the dispersion maps of *COF* can help for avoiding them.

3.2 Stribeck-like curves

Figure 7 presents the COF_e and COF_a values in Stribeck-like curves (all results except those for CV > 10). As expected, the *COF* values presented a reduction tendency increasing the Stribeck value, consonant with the hydrodynamic lubrication theory. For the testing conditions performed here, the lubrication regimes vary from boundary to mixed (do Vale *et al.*, 2019). Moreover, a better agreement for the COF_e (i.e. a higher value of R^2 and less dispersed points – mainly for the higher Stribeck values) could be noted. This better fit can be associated mainly with two reasons.

Figure 7 Stribeck-like curves

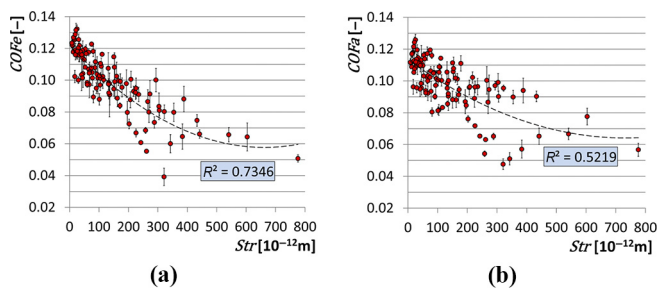

Notes: (a) COF_e; (b) COF_a

First, the V_i always presents null values at the reversal points (Figure 2), imposing a boundary lubrication regime at these regions. In the mid-stroke, however, the sliding velocity reaches its maximum value, meaning that the mixed lubrication regime is achieved. In addition, the Stribeck parameter [equation (5)] is based on this maximum velocity in an attempt to characterize a specific test condition. Therefore, while the *COF* values along the entire stroke gain in ease of calculation, they lose exactly in the representativeness regarding the lubrication regime, since all COF_i data are taken into account. As the COF_i values are much more significant in the COF_e formulation (Section 3.1) at the mid-stroke, a better fit using this definition is expected in the Stribeck-curves.

The second point is related to the advantage of the COF_e formulation in minimizing the perturbations caused by the acceleration, which to the Stribeck parameter, more critical for its higher values. A direct consequence of this is the relative lower COF_e dispersion for Str > 200.

Considering that the testing conditions imposed lubrication regimes from boundary to mixed, note that the R^2 coefficients shown in Figure 7 differs in 41 per cent, higher for the COF_e. Nonetheless, when the results are evaluated separately, the R^2 of the COF_e is 78.4 per cent higher for Str < 200 (i.e. lubrication regime closest to the boundary) and 79.8 per cent higher for Str > 200. This shows that the COF_e is even more effective for describing each lubrication regime separately.

4. Conclusions

Lubricated tests were performed under a reciprocating motion for a ring-on-cylinder configuration, describing two different approaches for determining the COF. The energetic approach minimizes the critical perturbations associated with the reversal points, where the acceleration has a significant effect on friction data. Based on the obtained results, the following conclusions can put forward:

- The statistical equality between COF_e and COF_a, found for the vast majority of tests (73.33 per cent), evidence that COF_e is not a new parameter for *COF* description, but rather it means a more robust formulation that minimizes the perturbations imposed by the reciprocating test itself.
- The values of the COF_e are larger than that observed for the COF_a in specific testing conditions, especially for the low frequencies and small tracks, although their reproducibility are similar.
- The use of the energetic approach for the friction resulted in a better description for a Stribeck-like curve, independent on the experienced lubrication regime along the stroke.
- The proposed COF_e parameter is a more robust alternative and had better representativeness, than COF_a, for reciprocating tests.
- The interpretation of friction results obtained in a reciprocating system should consider the level of perturbations at the reversal points.

References

Dimkovski, Z., Tomanik, E., Grange, S. and Epinat, F. (2018), "Novel testing methods for screening the tribological performance of ring-liner surfaces", *Surface Topography: Metrology and Properties*, Vol. 6 No. 3, p. 34017.

do Vale, J.L., da Silva, C.H. and Pintaúde, G. (2017), "Effect of graphite on folded metal occurrence in honed surfaces of grey and compacted cast irons", *Surface Topography: Metrology and Properties*, Vol. 5 No. 3, p. 35001.

do Vale, J.L., da Silva, C.H. and Pintaude, G. (2019), "Tribological performance assessment of lamellar and compacted graphite irons in lubricated ring-on-cylinder test", *Wear*, Vol. 426, pp. 471-480.

Holmberg, K., Andersson, P. and Erdemir, A. (2012), "Global energy consumption due to friction in passenger cars", *Tribology International*, Vol. 47, pp. 221-234.

Holmberg, K. and Erdemir, A. (2017), "Influence of tribology on global energy consumption, costs and emissions", *Friction*, Vol. 5 No. 3, pp. 263-284.

Kalin, M., Oblak, E. and Akbari, S. (2016), "Evolution of the nano-scale mechanical properties of tribofilms formed from low-and high-SAPS oils and ZDDP on DLC coatings and steel", *Tribology International*, Vol. 96, pp. 43-56.

Maru, M.M. and Tanaka, D.K. (2007), "Consideration of stribeck diagram parameters in the investigation on wear and friction behavior in lubricated sliding", *Journal of the Brazilian Society of Mechanical Sciences and Engineering*, Vol. 29 No. 1, pp. 55-62.

Spikes, H. (2004), "The history and mechanisms of ZDDP", *Tribology Letters*, Vol. 17 No. 3, pp. 469-489.

Tomanik, E. (2008), "Friction and wear bench tests of different engine liner surface finishes", *Tribology International*, Vol. 41 No. 11, pp. 1032-1038.

Vale, J.L., Guesser, W.L., Silva, C.H. and Pintaude, G. (2018), "Evaluation of friction coefficient of lamellar and compacted graphite irons in lubricated ring-on-cylinder system", SAE Technical Paper 2018-36-0058.

Corresponding author

Giuseppe Pintaude can be contacted at: giuseppepintaude@gmail.com